

Tracking gas-liquid coexistence in fluids of charged soft dumbbells

Heiko Braun and Reinhard Hentschke*

Fachbereich Mathematik und Naturwissenschaften, Bergische Universität, D-42097 Wuppertal, Germany

(Received 22 June 2009; revised manuscript received 27 August 2009; published 2 October 2009)

The existence of gas-liquid coexistence in dipolar fluids with no other contribution to attractive interaction than dipole-dipole interaction is a basic and open question in the theory of fluids. Recent Monte Carlo work by Camp and co-workers indicates that a fluid of charged hard dumbbells does exhibit gas-liquid (g-l) coexistence. This system has the potential to answer the above fundamental question because the charge-to-charge separation, d , on the dumbbells may be reduced to, at least in principle, yield the dipolar fluid limit. Using the molecular-dynamics technique we present simulation results for the g-l critical point of charged soft dumbbells at fixed dipole moment as function of d . We do find a g-l critical point at finite temperature even at the smallest d value (10^{-4}). Reversible aggregation appears to play less a role than in related model systems as d becomes small. Consequently attempts to interpret the simulation results using either an extension of Flory's lattice theory for polymer systems, which includes reversible assembly of monomers into chains, or the defect model for reversible networks proposed by Flusty and Safran are not successful. The overall best qualitative interpretation of the critical parameters is obtained by considering the dumbbells as dipoles immersed in a continuum dielectric.

DOI: [10.1103/PhysRevE.80.041501](https://doi.org/10.1103/PhysRevE.80.041501)

PACS number(s): 64.70.F-, 82.35.-x, 05.50.+q, 61.20.Qg

I. INTRODUCTION

The existence of a gas-liquid (g-l) critical point in systems consisting of particles whose sole source of mutual attraction is dipole-dipole interaction is an open question [1]. Roughly a decade ago a number of theoretical papers appeared predicting the absence of a g-l critical point in such dipolar systems due to the formation of reversible chains with essentially no mutual interaction [2–5]. This conclusion is in agreement with a number of computer simulation results obtained for dipolar systems. Caillol [6] searched without success for the g-l transition in systems of dipolar hard spheres (DHS) using NPT- (constant particle number, pressure, and temperature) and Gibbs-Ensemble-Monte Carlo (for temperatures larger than 0.18 and densities larger than 0.1). His search was motivated by an early Monte Carlo study of a 32-particle DHS system, claiming that the system undergoes g-l phase separation [7]. Van Leeuwen and Smit [8] studied a modification of the Stockmayer potential [Lennard-Jones (LJ) plus dipole-dipole], where the dispersion attraction is multiplied by a factor λ . In the limit $\lambda \rightarrow 0$ the model reduces to the dipolar soft sphere (DSS) potential. For λ less than a certain threshold van Leeuwen and Smit concluded that g-l criticality is absent due to chain formation. At the same time Stevens and Grest [9] studied the DSS system in an applied field. Whereas for nonzero field strengths they do observe coexistence; their conclusion in the zero field-case is that coexistence most likely does not occur. Szalai *et al.* [10] used computer simulation to investigate thermodynamics and structural properties of the dipolar Yukawa hard sphere (DYHS) fluid. They found that at high dipole moments the g-l coexistence disappears while chainlike structures appear in the low-density fluid phase. Recent molecular-dynamics

(MD) simulations of the Stockmayer fluid, which may be mapped onto the system studied by van Leeuwen and Smit, show that even though the threshold found in Ref. [8] does not exist, the conclusion that chain formation indeed leads to the disappearance of g-l criticality in the DSS limit still appears to be valid [11,12].

On the other hand other researchers, in addition to the aforementioned study by Ng *et al.* [7], have reached the opposite conclusion. McGrother and Jackson [13] induced g-l coexistence in a hard-core dipolar system by making the molecules nonspherical, i.e., they consider hard spherocylinders with central longitudinal point dipole moments. DHS are again studied via Monte Carlo in Ref. [14] by Camp *et al.* Based on their calculation of the equation of state and the free energy the authors found evidence in favor of an isotropic fluid-to-isotropic fluid phase transition. Pshenichnikov and Mekhonoshin [15] applied Monte Carlo to simulate DHS using open boundaries. Applying an extra field which confines the particles to a spherical region they observe a gaslike distribution within this region or a pronounced clustering depending on the strength of dipolar interaction. They interpret this as indication for phase separation in the DHS bulk system. Ganzenmüller and Camp [16] track the g-l coexistence which they find in systems of charged hard dumbbells (CHDs) as the dumbbells length is decreased toward the DHS limit. Via extrapolation of their Monte Carlo results obtained for finite dumbbell length they find a g-l critical point in the DHS limit. Almarza *et al.* [17] used Monte Carlo to investigate a mixture of hard spheres and DHS. They find critical parameters for the g-l equilibrium extrapolated from their mixture results in the limit of vanishing neutral hard sphere concentration in accord with the extrapolation results in Ref. [16] when the dumbbells approach the DHS limit. Kalyuzhnyi *et al.* [18] used Monte Carlo to study the g-l coexistence in the DYHS fluid. Again the critical point may be tracked as the DHS limit is approached by decreasing the strength of the attractive Yukawa potential. These authors find a critical point for values of the control parameter rep-

*Author to whom correspondence should be addressed; hentschk@uni-wuppertal.de

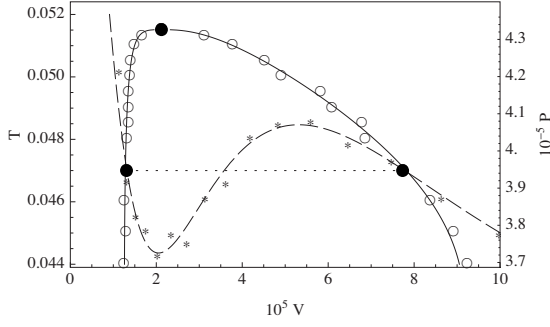


FIG. 1. Example section of a simulated isotherm (stars) including the attendant coexistence densities (solid circles) as well as those of additional isotherms not explicitly shown (hollow circles). All data are based on a CSD system with $d=10^{-3}$. The isotherm is for $T=0.047$. Dashed line: fit to the entire isotherm obtained using an empirical equation of state; dotted line: equal area construction; solid line: fit to the coexisting densities via the scaling relations (9) and (10). Single solid circle: critical point.

representing the “distance” from the DHS limit which are far lower than the limit set by the earlier study in Ref. [10]. Continuation of this work in Ref. [1] however results in the conclusion that phase separation is not observable beyond a critical value of the aforementioned parameter.

Tracking the g-l critical point in a system approaching the dipolar hard or dipolar soft sphere limit by changing an appropriate parameter has a particular appeal. One may begin the simulation in an “easy regime” where g-l phase separation is readily observed. Subsequently the DHS or DSS limits are approached in such a way that difficulties, basically reversible association of particles, develop “slowly,” enabling extrapolation to the desired limit. In this work we study a system of charged soft dumbbells (CSD) using the molecular-dynamics technique. The charge-to-charge separation, d , is systematically decreased, keeping the dipole moment constant. Even at the smallest d (10^{-4}) we do observe a transition terminating in a critical point. Interpretation of the critical behavior in terms of different simple models is attempted. However, neither the extension of Flory’s lattice theory to reversibly aggregating polymers [19,20] nor the defect model put forward by Tlustý and Safran (TS) [21] yields a consistent description of the simulation results. The simulations therefore strongly suggest a g-l critical point in the limit of dipolar soft spheres, which is in line with the previous simulation study by Ganzenmüller and Camp [16] for dipolar hard spheres.

The paper is structured as follows. Subsequent to this introduction we discuss the model in Sec. II. Section III contains the details of our simulation approach. The results Sec. IV discusses first the dependence of the g-l critical parameters of a fluid of Lennard-Jones dumbbells and subsequently the analogous behavior in the charged soft dumbbell system. Section V is the conclusion.

II. MODEL

We consider a fluid of charged soft dumbbells. Each dumbbell consists of two opposite charges of magnitude q

with fixed distance d . Each charge site interacts with charge sites on other dumbbells via a r^{-12} repulsive potential in addition to their Coulomb interaction. The dumbbell-dumbbell potential energy is given by

$$u_{ij} = \sum_{\alpha,\beta=1}^2 \left(\frac{4}{r_{i\alpha j\beta}^{12}} + \frac{q_\alpha q_\beta}{r_{i\alpha j\beta}} \right). \quad (1)$$

Here the indices i and j denote distinct dumbbells, whereas α and β refer to the charge sites on dumbbell i and j , respectively. The leading terms in the multipole expansion of u_{ij} are

$$u_{ij} \approx \frac{4}{r_{ij}^{12}} + \frac{\mu^2}{r_{ij}^3} (\vec{n}_i \cdot \vec{n}_j - 3(\vec{e}_{ij} \cdot \vec{n}_i)(\vec{e}_{ij} \cdot \vec{n}_j)) - \frac{\mu^2 d^2}{8r_{ij}^5} \times (6\vec{n}_i \cdot \vec{n}_j - 15(\vec{e}_{ij} \cdot \vec{n}_i)(\vec{e}_{ij} \cdot \vec{n}_j) - [(\vec{e}_{ij} \cdot \vec{n}_i)^2 + (\vec{e}_{ij} \cdot \vec{n}_j)^2](15\vec{n}_i \cdot \vec{n}_j + 35(\vec{e}_{ij} \cdot \vec{n}_i)(\vec{e}_{ij} \cdot \vec{n}_j))), \quad (2)$$

where r_{ij} is the center of mass separation between the dumbbells and \vec{e}_{ij} is a unit vector on the line joining the two centers of mass pointing toward the center of mass of dumbbell i . In addition $\mu=dq$ (here: $\mu=1$) and \vec{n}_i is a unit vector on the line joining the charges in dumbbell i pointing from the negative to the positive charge. In the limit $d \rightarrow 0$ the interaction therefore reduces to the DSS potential consisting of the r^{-12} repulsion plus the interaction between point dipoles.

III. SIMULATION METHODOLOGY

We carry out MD simulations in the NVT ensemble. Notice that the equations of motion for a dumbbell are given by $d\vec{P}/dt = \vec{f}_1 + \vec{f}_2$ and $d\vec{L}/dt = \vec{N}$. Here \vec{P} and \vec{L} are the total linear and rotational momentum, respectively. \vec{f}_i denotes the total force on site i of the dumbbell. \vec{N} is the total torque. We may choose to rewrite the above in term of Euler’s equations. The angular equations are equivalent to Eq. (A6) for the rotational motion of the unit vector \vec{n} , here along the connecting line between the charge sites on a dumbbell, in Ref. [22], i.e.,

$$\ddot{\vec{n}}_i = \vec{G}_i - [\vec{n}_i \cdot \vec{G}_i + (\dot{\vec{n}}_i)^2] \vec{n}_i, \quad (3)$$

where $\vec{G}_i = -\mathcal{I}^{-1}(\partial U / \partial \vec{n}_i)$. The details of the derivation may be found in the aforementioned reference as well as in Sec. 8.2. of Ref. [23].

In LJ units \mathcal{I} , the moment of inertia with respect to the momentary axis of rotation is $\mathcal{I} = d^2/2$. In order to obtain the usual dipolar soft sphere limit we also use $\mathcal{I} = 1$. The equations of motion for translation and rotation are integrated via the velocity Verlet algorithm with a suitable time step. The length of the \vec{n}_i is adjusted to unity every time step to avoid numerical inaccuracies. The simulations are performed using the weak coupling method of Berendsen *et al.* [24]. Notice that in the present units the rotational temperature is $T_{rot} = (\mathcal{I}/2)\langle \dot{\vec{n}}_i^2 \rangle$. The thermalization of the $\dot{\vec{n}}_i$ is implemented analogous to the thermalization of the translational motion.

The dumbbells are initially arranged on a fcc lattice and assigned random velocities. Typically individual MD runs

consist of 50–250 LJ time units of equilibration and 200–1000 time units of production per state point. Along the same isotherm runs at a new density are started from the final configuration of the preceding density. The time step varies from 10^{-3} for $\mathcal{I}=1$ to 10^{-5} for $\mathcal{I} \neq 1$.

Forces originating from short-range potentials are computed using the minimum image convention applied to the individual interaction sites. The cutoff distance is $r_{cut}=10$ unless noted otherwise. Beyond the cutoff we apply the usual corrections to pressure and internal energy again based on the individual interaction sites. Coulomb interaction are computed using a residue cutoff, i.e., the entire dumbbell is included in the calculation if the condition

$$\min_{\alpha,\beta} [r_{i_\alpha j_\beta}] \leq r_{cut} = 10 \quad (4)$$

is fulfilled. Beyond r_{cut} we apply the reaction field (RF) method [25] as described by Tironi *et al.* [26]. The RF contributes to the force on dumbbell i via

$$\vec{F}_i^{RF} = \frac{2(\epsilon-1)}{2\epsilon+1} \frac{1}{r_{cut}^3} [q_{i_1} \vec{M}_{i_1} + q_{i_2} \vec{M}_{i_2}], \quad (5)$$

where ϵ is the dielectric constant of the fluid and \vec{M}_{i_α} is the dipole moment of the cutoff sphere centered on site i_α . In

general we have $\vec{F}_i^{RF} \neq 0$ as the spheres around the sites on the same dumbbell are not identical. In addition to the force the RF also has an effect on the torque on dumbbell i with orientation \vec{n}_i , i.e.,

$$\vec{N}_i^{RF} = \frac{2(\epsilon-1)}{2\epsilon+1} \frac{1}{r_{cut}^3} \frac{d}{2} \vec{n}_i \times [q_{i_1} \vec{M}_{i_1} - q_{i_2} \vec{M}_{i_2}]. \quad (6)$$

The unknown dielectric constant ϵ can be obtained via

$$\frac{(\epsilon-1)(2\epsilon+1)}{3\epsilon} = \frac{\langle \vec{M} \cdot \vec{M}_{Box} \rangle}{Tr_{cut}^3} \quad (7)$$

with the dipole moment of a cutoff sphere \vec{M} and the total dipole moment of the simulation box \vec{M}_{Box} . Equation (7) is evaluated at each simulation step. The calculation of the RF contribution to force and torque is based on the cumulative average of ϵ .

Phase coexistence is established using the Maxwell construction method applied to simulation isotherms at different temperatures. This approach was applied previously to g-l coexistence in the Stockmayer fluid as well as another pseudodipolar model fluid and the details are discussed elsewhere [11,22]. An example is shown in Fig. 1. In the present case the pressure is computed via

$$P = P_{ideal} + \frac{1}{3V} \left\langle \sum_{i < j}' \vec{r}_{ij} \cdot \vec{f}_{ij} \right\rangle + \frac{1}{3V} \left\langle \frac{d}{2} \sum_{i < j}^N [(\vec{n}_i + \vec{n}_j) \cdot (\vec{f}_{i_2 j_1} - \vec{f}_{i_1 j_2}) + (\vec{n}_i - \vec{n}_j) \cdot (\vec{f}_{i_2 j_2} - \vec{f}_{i_1 j_1})] \right\rangle. \quad (8)$$

In the second term the sum is over all site pairs excluding (prime) sites on the same dumbbell. In the third term the sum is over pairs of dumbbells. Note that the orientation of \vec{n} is toward site 1. The critical parameters are obtained via application of the following scaling relations [27] using Ising critical exponents ($\alpha \approx 0.110$, $\beta \approx 0.326$, $\Delta \approx 0.5$ [28]):

$$\rho_F - \rho_G \approx A_0 |t|^\beta + A_1 |t|^{\beta+\Delta}, \quad (9)$$

$$(\rho_F + \rho_G)/2 \approx \rho_c + D_0 |t|^{1-\alpha} + D_1 |t|, \quad (10)$$

$$P - P_c \approx P_0 |t| + P_1 |t|^{2-\alpha} + P_2 |t|^2. \quad (11)$$

Here $t = (T - T_c)/T_c$.

IV. RESULTS

In order to make contact with previous work on uncharged LJ dumbbells we study the g-l critical behavior of the pair potential

$$u_{ij}^{(LJ)} = \sum_{\alpha,\beta=1}^2 \left(\frac{4}{r_{i_\alpha j_\beta}^{12}} - \frac{4}{r_{i_\alpha j_\beta}^6} \right). \quad (12)$$

In all cases the number of dumbbells is 500, $r_{cut}=3.5$, and $\mathcal{I}=d^2/2$. Figure 2 summarizes the critical parameters for this

system including comparisons to results taken from the literature. The dashed lines in Fig. 2 (top and middle panel) correspond to $\rho_c(d) = \rho_c^o v_s / v_{sc}$ and $T_c(d) = T_c^o (v_s / v_{sc})^2$. Here ρ_c^o and T_c^o are the values of the critical parameters obtained by us for $d=10^{-4}$. $v_{sc}/v_s = 1 + 3d/4$ is the volume of a spherocylinder with cylinder length d divided by the volume of a sphere with identical radius (equal to one). This shows that most of the decrease seen for ρ_c and T_c with increasing d is accounted for by van der Waals theory, i.e., $P = T\rho/(1 - b\rho) - a\rho^2$ with $\rho_{c,vdW} \propto 1/b$ and $T_{c,vdW} \propto a/b$. Obviously $b \propto v_{sc}/v_s$, but the same dependence on dumbbell volume is expected also for a^{-1} , i.e., $a \propto (v_{sc}/v_s)^{-1}$. Here we argue that the attractive long-range contribution to the pressure in a system with radial r^{-6} interaction between particles is proportional to $\rho^2 r_{cut}^{-3}$. If we roughly associate r_{cut}^3 with the volume of the particles we arrive at the above dependence of a on v_{sc}/v_s . Long spherocylinders do not approximate the dumbbells very well. This is why we limit our simple approximation to $d < 1.5$. For large d both ρ_c and T_c approach constant values as one might expect. Notice that $T_c(d)$ is bracketed by $4T_{c,LJ}$ at $d=0$ and $T_{c,LJ}$ at large d . At $d=0$ the two dumbbell sites fuse into one single LJ site, thereby quadrupling the number of interactions between these effective LJ sites. At large d each dumbbell site approximately behaves as independent LJ particle. Finally we note that the

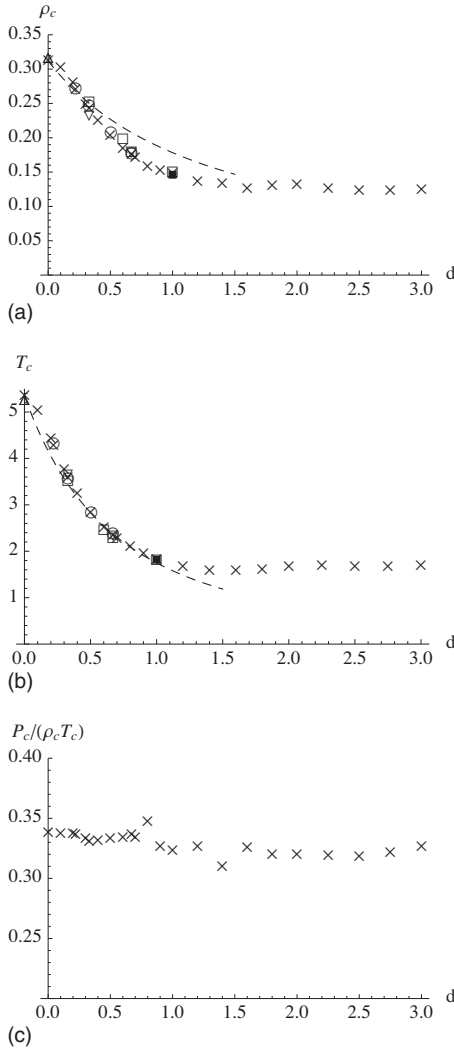


FIG. 2. Critical density, ρ_c (top), critical temperature, T_c (middle), critical compressibility factor, $P_c/(\rho_c T_c)$ (bottom), of LJ dumbbells vs d . Crosses: this work; circles: [29]; down-triangles: [30]; squares: [31]; up-triangle: [32]; solid square: [33]. The dashed lines are explained in the text.

critical compressibility factor shown in the bottom panel of Fig. 2 is constant within the scatter of the result, in agreement with the above reasoning based on van der Waals-like theory.

We now turn to the charged dumbbells. Here all simulations are for 800 dumbbells. In the following figures crosses are results obtained with $\mathcal{I}=d^2/2$ and circles correspond to $\mathcal{I}=1$. The symbols in Fig. 3 represent the critical parameters obtained via simulation versus d . We observe that the results obtained with $\mathcal{I}=d^2/2$ show more scatter than those for fixed moment of inertia. The former case is numerically more demanding due to the larger average velocity of rotation at small d in comparison to dumbbells with fixed moment of inertia. Deviations between the two cases, in particular for the critical density, are due to differences in the size distribution of reversible aggregates formed by the dumbbells. Larger average rotational velocity tends to make the dumbbell-dumbbell interaction less anisotropic on average, which in turn reduces aggregation (cf. below) [34]

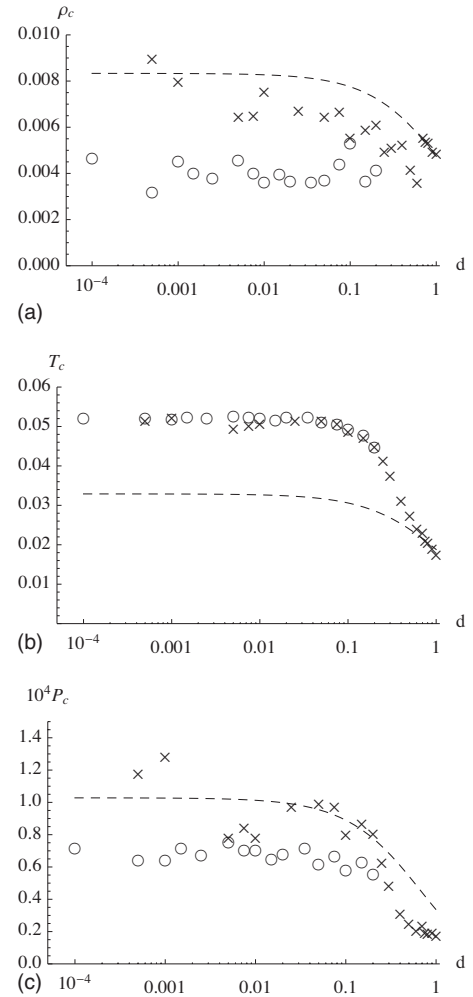


FIG. 3. Critical density, ρ_c (top), critical temperature, T_c (middle), and critical pressure, P_c (bottom), vs d . Symbols: simulation (circles: fixed moment of inertia; crosses: d -dependent moment of inertia); dashed lines: mean field result (Onsager's reaction field approach).

The most important result is that the critical parameters approach finite values for $d \rightarrow 0$, i.e., in the limit of dipolar soft spheres. It is interesting to compare these limiting values to previous corresponding results for dipolar hard spheres. Here we compute an effective hard-core diameter, $\sigma_{eff}(T)$, via $B_2(T) \approx B_2(\text{HS}) = 4(\pi/6)\sigma_{eff}^3$, where $B_2(\text{HS})$ is the second virial coefficient of hard spheres and $B_2(T)$ is the second virial coefficient of soft spheres at temperature T . The result is $\sigma_{eff}(T) = [\Gamma(3/4)]^{1/3} (4/T)^{1/12}$ ($[\Gamma(3/4)]^{1/3} \approx 1.07011$; note that the corresponding result using the Barker-Henderson formula [35] is $\sigma_{eff}(T) \approx 1.0555(4/T)^{1/12}$). Multiplication of the critical temperature in the limit $d \rightarrow 0$, i.e., $T_c \approx 0.052$, with $\sigma_{eff}(T_c)^3$ yields 0.18. This number is to be compared to the range of $T_c \sigma^3$ values obtained for dipolar hard spheres in the aforementioned references [16,18] between 0.15 to 0.17 (note: $\mu=1$). Similarly we may map the critical density in the limit $d \rightarrow 0$, i.e., $\rho_c \approx 0.004$ to 0.008, to the hard sphere case via $\sigma_{eff}^3 \rho_c$, which yields 0.014 to 0.028. The corresponding literature range of the same quantity for DHS is 0.05 to 0.1. Certainly, this type of mapping usually is quite crude. Nevertheless the consistency is apparent.

In an attempt to explain the simulation data we first construct a mean field theory ignoring possible association of the dumbbells into reversible aggregates. We consider a modified van der Waals free energy $f = \Delta F / (NT)$ given by

$$f = \ln \frac{b\rho}{1-b\rho} - \frac{4\pi}{3} \frac{\epsilon - 1}{2\epsilon + 1} \frac{\mu^2}{bT}. \quad (13)$$

The first term in Eq. (13) is the usual van der Waals repulsion. The second term is the free energy of immersion of a point dipole μ in a spherical cavity of volume b in a medium with dielectric constant ϵ [25]. Here of course we assume

$$b = b_o(1 + 3d/4), \quad (14)$$

akin to the above discussion of LJ dumbbells. The dielectric constant is given by

$$\frac{1}{4\pi} \frac{(\epsilon - 1)(2\epsilon + 1)}{\epsilon} = \frac{\rho\mu^2}{T}. \quad (15)$$

Because we expect the critical point at low densities we may expand ϵ in terms of ρ . Keeping first-order terms only we obtain the critical parameters

$$\rho_c \approx \frac{1}{3b} \quad T_c \approx \frac{8\sqrt{2}\pi\mu^2}{27b} \quad P_c \approx \frac{\sqrt{2}\pi\mu^2}{27b^2}, \quad (16)$$

and $P_c / (\rho_c T_c) \approx 3/8$. Notice that in the LJ case we may use $b_o \approx 1$, based on fitting the van der Waals equation to near critical isotherms. This yields $\rho_c(d=0) \approx 1/3$, in accord with the simulation result in Fig. 2. In the case of the CSD we may estimate b_o via the second virial coefficient of the $4/r^{12}$ potential at $T \approx 0.05$, i.e., $b_o \approx 8$ and therefore $\rho_c \approx 0.04$. This exceeds the simulation results (for fixed moment of inertia) by a substantial factor (see Fig. 3). The large factor indicates that, in contrast to the LJ system, the assumption of isolated dumbbell particles is not correct and that reversible aggregation occurs. Below we discuss simulation results showing an average aggregation number close to 5 for small d . Using $b_o \approx 40$ we obtain the dashed lines in Fig. 3. Even though not quantitatively accurate the emerging picture appears to qualitatively represent the simulation results. In particular the theory yields an initial increase in all critical quantities with decreasing d akin to the d effect seen for the LJ dumbbells. Notice also that here $T_c \propto (1 + 3d/4)^{-1}$ rather than $\propto (1 + 3d/4)^{-2}$ as in the case of LJ dumbbells. This is because the van der Waals attraction parameter in the case of the dipoles (at low concentration) is given by $a = (4\pi/3)^2 [\mu^4 / (3bT)]$. Thus there is a temperature dependence which is absent in case of the LJ system.

A likely form of clustering is the formation of reversible chains or network frequently observed in dipolar systems [36]. The effect chain formation has on the critical parameters may be understood via Flory's equation of state [37], i.e.,

$$\frac{bP}{T} = - \left(1 - \frac{1}{n} \right) \phi - \ln[1 - \phi] - \frac{q\epsilon_o}{2T} \phi^2, \quad (17)$$

derived on the basis of a lattice description of the packing entropy of linear chains consisting of n segments. Note that q

is the coordination number of the lattice. Here $\phi = b\rho$ is the chain volume fraction and b is the monomer or segment volume. The resulting critical parameters are $\rho_c = b^{-1} (1 + \sqrt{n})^{-1}$ and $T_c = T_c^\infty n (1 + \sqrt{n})^{-2}$ with $T_c^\infty = T_{\text{Boyle}} = -q\epsilon_o$. Here T_{Boyle} is the Boyle temperature for the case $n=1$. In the case $n=1$, i.e., monomers instead of chains, both ρ_c and T_c are very similar to the van der Waals critical parameters. However, for large n we observe that the critical density vanishes as $\rho_c \sim n^{-1/2}$ [38] and T_c rises toward a constant value.

In the present case n is not a constant. The dumbbells may aggregate reversibly into linear chains (ignoring junction formation for the moment). It turns out that the above equation of state still holds if n is identified with the number-averaged chain size [20]. In the low concentration limit, i.e., chain-chain interaction is ignored, this average length is given by

$$n = \frac{1}{2} + \frac{1}{2} \sqrt{1 + 4(q-1)\phi e^{-\epsilon_i}}. \quad (18)$$

The quantity ϵ_i is an in-chain contact free energy. This formula is well known from the theory of micellar systems (see for instance Ref. [39]). Inserting this expression into Eq. (17) yields modified critical parameters, i.e.,

$$\rho_c = \frac{1}{b} \left(1 + \sqrt{\frac{m^3}{K}} \right)^{-1} \quad T_c = -\frac{1}{2} q\epsilon_o \left\{ \frac{n}{m} + [K - n(n-1)] \sqrt{\frac{1}{Km^3}} \right\}^{-1}, \quad (19)$$

where $m = 2n - 1$ and $K = 6n(n-1) + 1$. Even though these expressions are considerable more messy than those for constant n , the limiting n dependence for large n remains unaltered, i.e.,

$$\rho_c \approx \frac{1}{b} \frac{\sqrt{3}}{2} \frac{1}{n_c^{1/2}} \quad T_c \approx -q\epsilon_o \quad P_c \approx -\frac{q\epsilon_o}{b} \frac{5\sqrt{3}}{16} \frac{1}{n_c^{3/2}}. \quad (20)$$

Here $n_c = n(\phi_c, \epsilon_i(T_c))$. This means that in the case of unlimited chain growth as d approaches zero, we can expect the critical density to vanish. The fate of the critical temperature depends on a possible d dependence of ϵ_o , which is *a priori* unknown. However, the critical compressibility factor should scale as $P_c / (\rho_c T_c) \sim n_c^{-1}$, independent of adjustable parameters like b or ϵ_o . Figure 4 shows the critical compressibility factor versus d . After an initial increase as d is decreased from unity, $P_c / (\rho_c T_c)$ remains constant at a value which is in line with the prediction of the above mean field theory of dipoles immersed in a continuum dielectric. This indicates that aggregation at small d occurs but is limited to rather small aggregation numbers.

The number average size, n , of the reversible aggregates as function of d is shown in Fig. 5. Here n is determined via a distance criterion. Two dumbbells are considered to belong to the same cluster or aggregate if the separation between any of their charge sites to any of the charge sites on another dumbbell is less than 2. Of course changing this number will change n (keeping d constant) to some extent, but the basic dependence of n on d remains unaltered. We observe that n

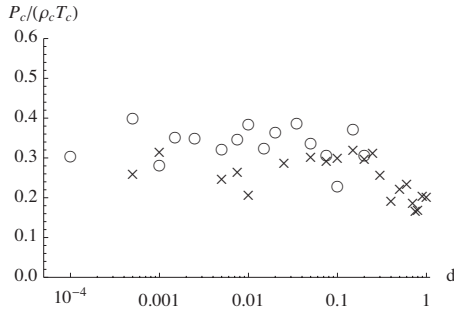


FIG. 4. Critical compressibility factor vs d . Symbols: as in previous figure.

on average is reduced as d becomes smaller. In the range $10^{-4} < d < 10^{-1}$ no effect of d on n is observed. This plateau value corresponds to $n \approx 5$.

Two selected examples of the aggregate size distribution for $\rho=0.006$ and T close to the respective T_c are shown in Fig. 6. Here reversible aggregation means that we may employ the chemical equilibrium condition $\mu_s = s\mu_1$, where the s -mer chemical potential (at low concentration) is $\mu_s = \bar{\mu}_s + T \ln X_s$. Therefore $X_s = (X_1 e^{\alpha})^s$, where X_s is the mole fraction of s -mers, $\alpha = (\bar{\mu}_1 - \bar{\mu}_s/s)/T = (\bar{\mu}_1 - \bar{\mu}_{\text{bulk}})/T - \delta s^{-1/D}$ (D : space dimension; $D=1$ for chainlike aggregates), and $T\delta$ is a surface free enthalpy [40]. The linear behavior of the simulation data in the bottom panel of Fig. 6 over a significant s range attest to the applicability of this aggregation model for small d . The corresponding data for $d=1$, however, indicates that for large d the aggregates are not predominantly linear. Figure 7 shows corresponding configuration snapshots.

In summary we observe rather broad aggregate size distributions. The average size however is small (around 5) for

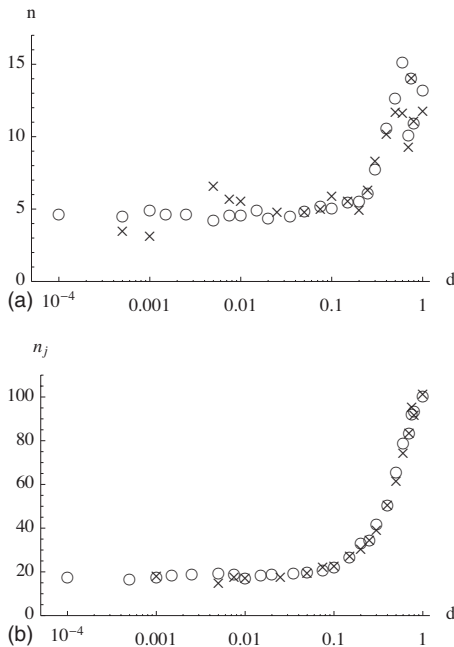


FIG. 5. Average aggregation number, n (top), corresponding average number of junctions per configuration, n_j (bottom), vs d for $\rho=0.006$ and $T \approx T_c$. The meaning of the symbols is the same as in Fig. 3.

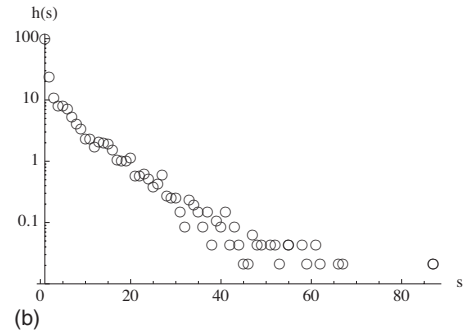
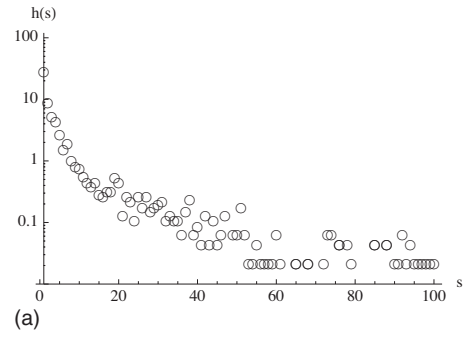


FIG. 6. Aggregate size distribution, frequency $h(s)$ vs s , at $\rho = 0.006$ for T close to the respective T_c . Top: $d=1$; bottom $d = 0.001$.

$d > 0.1$. The above theory, which explains the shift of the critical parameters rather well in the Stockmayer [11,20] and another dipolar model fluid [22], where long chains are formed, does not come to bear in the present case because n remains rather small. Notice that chain growth, according to Eq. (18), is driven by concentration and the in-chain contact free energy ε_i . In the present case the charges on a dumbbell do retreat into the center of the soft-repulsive core as d decreases. Thus if $d \ll 1$ there is no obvious reason why $-\varepsilon_i$ should increase, and therefore the average size, n , approaches a constant at constant particle density and constant magnitude of the dipole moment.

Thus far we have discussed implications of chain formation. Configuration snapshots like the one shown in Fig. 7

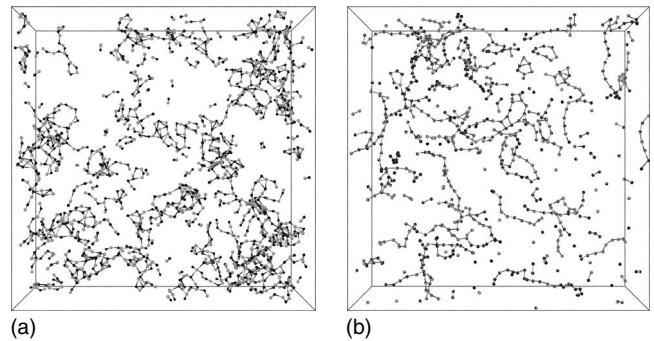


FIG. 7. Simulation snapshots corresponding to the aggregate size distributions shown in the previous figure. Top: $d=1$; bottom: $d=0.001$. Differently shaded spheres correspond to positive and negative charges, respectively. Uniform gray lines are drawn between dumbbells at close proximity to highlight reversible aggregation.

(top) do reveal the possible presence of networklike structures—at least for the larger d values. In the following we therefore discuss possible implications of network formation.

An entirely different mechanism for phase separation in dipolar systems was suggested by Tlustý and Safran [21]. The model is based on the observation of network structures formed by reversible chains as found in dipolar systems. TS suggested the occurrence of phase coexistence between a free ends-rich/junction-poor and a free ends-poor/junction-rich phase instead of the usual g-l coexistence in simple liquids. The part of the free energy, derived in the framework of the self-consistent field approach to polymer systems [41], responsible for this transition consists of three contributions, i.e.,

$$f = -(2\phi)^{1/2}e^{-\epsilon_1/T} - \frac{1}{3}(2\phi)^{3/2}e^{-\epsilon_3/T} + \frac{1}{2}\phi^2. \quad (21)$$

Two terms describe the concentration of free chain ends and threefold network junctions as defects in a perfect network. The third is a simple excluded volume interaction proportional to the square of the monomer density. Associated with each type of defect are energetic costs, ϵ_1 (free ends) and ϵ_3 (threefold junctions). TS find that the free ends contribute an additional repulsion in the equation of state whereas the junctions contribute attraction. The resulting critical parameters are

$$T_c^{\text{TS}} = \frac{\epsilon_1 - 3\epsilon_3}{\ln[27/4]}, \quad (22)$$

$$\ln \phi_c^{\text{TS}} = - \frac{\epsilon_1 \ln[9/2] - \epsilon_3 \ln[2]}{\epsilon_1 - 3\epsilon_3}, \quad (23)$$

$$\ln P_c^{\text{TS}} = - \frac{\epsilon_1 \ln[81/2] - \epsilon_3 \ln[32]}{\epsilon_1 - 3\epsilon_3}. \quad (24)$$

Figure 8 (top) shows the defect energies, ϵ_1 and ϵ_3 , as obtained by inserting the simulation results for T_c and P_c (note that using T_c and ρ_c instead does change this result quantitatively by 10 to 20% but not qualitatively). It is sensible that the energetic cost of free ends is higher than that of junctions. Unfortunately a sufficiently precise computation of the defect energies ϵ_1 and ϵ_3 is difficult and a real obstacle to the application of the TS approach. The solid line shows a result obtained for ϵ_1 via the equation $U(n)/n = u_{\text{bulk}} + 2\epsilon_1 n^{-1}$ for large n . Here $U(n)$ is the potential energy of a straight chain of n CSD aligned head to tail. In addition the separation between the dumbbells is obtained via energy minimization. Around $d=1$ the agreement is reasonable, but for small d the deviation becomes considerable (the estimated ϵ_1 approaches a value close to 0.7 for $d \rightarrow 0$). ϵ_3 is even more difficult to compute reliably, because of numerous ambiguities associated with model junctions. This essentially prevents an “*ab initio*” computation of the critical parameters. Figure 8 (bottom) shows the density of junctions, ρ_3 , at the critical point obtained via the above theory, i.e., $\rho_3 \sim (\rho_c^{\text{TS}})^{3/2} \exp[-\epsilon_3/T_c^{\text{TS}}]$, with ρ_c^{TS} and P_c^{TS} substituted from the simulation. As d is decreased from one the junction den-

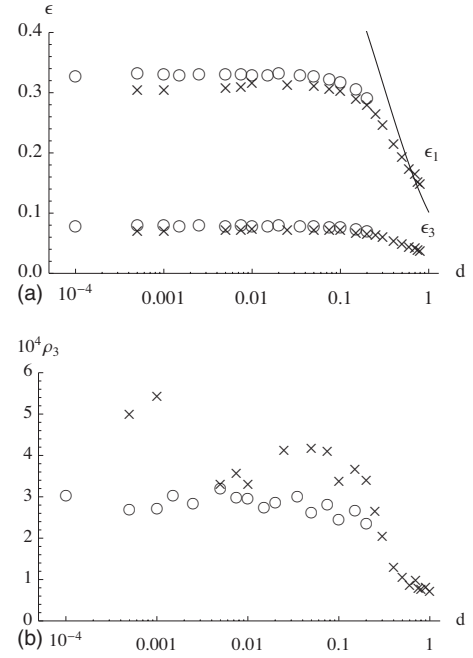


FIG. 8. Tlustý-Safran model. Top: Defect energies as obtained from the simulation results for T_c and P_c . The solid line is explained in the text. Bottom: concentration of junctions, ρ_3 vs d .

sity increases and reaches an (apparent) maximum value. Computing the junction concentration directly on the basis of simulated system configurations near criticality shows the opposite trend however [cf. Fig. 5 (bottom)]. In the simulation the junction concentration, a junction is defined via the requirement that a particle has more than two neighbors according to the above distance criterion, drops continuously as d decreases.

The main weaknesses of the TS approach, in our view, are the complete neglect of higher correlations and more importantly the exclusive description of a (dipolar) liquid in terms of chain ends or junctions thereof. While this is elegant it does not necessarily work. For instance the model does not include normal gas-liquid coexistence in terms of monomers or possibly chains [gas-liquid criticality of simple n -alkanes is described quite satisfactorily by the (Flory lattice) theory discussed above]. In essence we believe that in the present case the TS theory is an oversimplification and that the true driving force behind the observed phase separation is not just a competition of free ends vs junctions as assumed in the construction of the underlying partial free energy.

V. CONCLUSION

Qualitatively we obtain results for the g-l critical parameters in agreement with previous work on CHD in Ref. [16]. As the charge-to-charge separation d is reduced at constant dipole moment we find that even for the smallest d there is a g-l critical point [$\rho_c \approx 0.004$ (fixed moment of inertia) and $T_c \approx 0.05$]. We interpret the d dependence of the critical parameters in terms of three different models. A mean field model of isolated dipoles immersed in a dielectric continuum yields the qualitatively correct d dependence, even though

aggregate formation does prevent a more quantitative comparison. Interpretation of the data in terms of Flory's equation of state for linear polymers, where the fixed chain length is replaced by an average chain length of equilibrium polymeric chains, does not succeed because the reversible aggregates remain rather small. An attempt to correlate the observed behavior with the defect model due to Tlusty and Safran also fails because the number of network nodes, which should increase for $d \rightarrow 0$, based on the defect energies obtained via the simulated critical parameters, in this system decreases instead. In summary the first model offers the overall best basis for the understanding of the simulation data.

In a previous publication [12] we discuss the implications of the mapping that exists between the Stockmayer (ST) fluid, for which the g-l phase coexistence has been studied via molecular dynamics simulation in Refs. [11,20], and a second model consisting of a Lennard-Jones (LJ) potential with adjustable dispersion attraction in addition to the same dipole-dipole term as in the ST fluid. The latter model was studied via Gibbs-Ensemble Monte Carlo simulation by van Leeuwen and Smit [8]. The ST potential is given by

$$\frac{U_{\text{ST}}(r_{\text{ST}}, \mu_{\text{ST}})}{T_{\text{ST}}} = \frac{4}{T_{\text{ST}}} \left(\frac{1}{r_{\text{ST}}^{12}} - \frac{1}{r_{\text{ST}}^6} \right) - \frac{\mu_{\text{ST}}^2}{T_{\text{ST}} r_{\text{ST}}^3} f, \quad (25)$$

where f simply is a function of the relative orientation of two interacting dipoles. The quantities r_{ST} , μ_{ST} , and T_{ST} refer to interparticle separation, magnitude of the dipole moment, and temperature, respectively. The other potential, here denoted via van Leeuwen and Smit (vLS), is

$$\frac{U_{\text{vLS}}(r_{\text{vLS}}, \mu_{\text{vLS}})}{T_{\text{vLS}}} = \frac{4}{T_{\text{vLS}}} \left(\frac{1}{r_{\text{vLS}}^{12}} - \lambda \frac{1}{r_{\text{vLS}}^6} \right) - \frac{\mu_{\text{vLS}}^2}{T_{\text{vLS}} r_{\text{vLS}}^3} f, \quad (26)$$

where λ is a parameter. Notice that the vLS potential includes the dipolar soft sphere (DSS) potential in the limit $\lambda \rightarrow 0$. The two formulas for U/T may be converted into each other via the relations $T_{\text{ST}} = \lambda^{-2} T_{\text{vLS}}$, $\rho_{\text{ST}} = \lambda^{-1/2} \rho_{\text{vLS}}$, and $\mu_{\text{ST}} = \lambda^{-3/4} \mu_{\text{vLS}}$ (cf. Sec. II in Ref. [42]). Notice that $\exp[-U/T]$ determines configurational averages in the NVT ensemble. Thus we conclude that the Stockmayer fluid approaches the DSS system in the limit of infinite dipole moment μ_{ST} . All previous simulations obtaining g-l critical parameters of the Stockmayer fluid for large dipole moments support the finding that T_c in this regime is described very precisely via $T_{c,\text{ST}} = b + m \mu_{\text{ST}}^2$, where m and b are constants. (In Ref. [12] we find $m \approx 0.2587$ and $b \approx 1.0006$.) Using this equation we may convert $T_{c,\text{ST}}$ to $T_{c,\text{vLS}}$ via $T_{c,\text{vLS}} = \lambda^2 (b + m \lambda^{-3/2} \mu_{\text{vLS}}^2) = \lambda^2 b + \lambda^{1/2} m \mu_{\text{vLS}}^2$. Thus for $\lambda \rightarrow 0$ we find $T_{c,\text{vLS}} \rightarrow 0$, i.e., DSS should not show g-l phase separation. A finite $T_{c,\text{vLS}}$ in the limit $\lambda \rightarrow 0$ may be obtained via $T_{c,\text{ST}} = b + m \mu_{\text{ST}}^2 + c \mu_{\text{ST}}^{8/3}$, i.e., $T_{c,\text{vLS}} \rightarrow c$ as $\lambda \rightarrow 0$. This form has been tried but yields no acceptable c value when fitted to the simulation data (analogous to the previous fit procedure in Ref. [12]). In addition $\rho_{\text{vLS}} = \lambda^{1/2} \rho_{\text{ST}}$ predicts $\rho_{\text{vLS}} \rightarrow 0$ for $\lambda \rightarrow 0$, i.e., in the DSS limit, unless ρ_{ST} increases sufficiently as μ_{ST} is increased. All previous simulations (cf. Fig. 3 in Ref. [20]) find the contrary in the ρ_{ST} range studied thus far. This certainly remains a disturbing issue.

ACKNOWLEDGMENT

This work was supported by the German Science Foundation through DFG-Grant No. HE 1545/17-1.

-
- [1] G. Ganzenmüller, G. N. Patey, and P. J. Camp, *Mol. Phys.* **107**, 403 (2009).
- [2] R. P. Sear, *Phys. Rev. Lett.* **76**, 2310 (1996).
- [3] R. van Roij, *Phys. Rev. Lett.* **76**, 3348 (1996).
- [4] J. M. Tavares, M. M. Telo da Gama, and M. A. Osipov, *Phys. Rev. E* **56**, R6252 (1997).
- [5] Y. Levin, *Phys. Rev. Lett.* **83**, 1159 (1999).
- [6] J.-M. Caillol, *J. Chem. Phys.* **98**, 9835 (1993).
- [7] K.-C. Ng, J. P. Valleau, G. M. Torrie, and G. N. Patey, *Mol. Phys.* **38**, 781 (1979).
- [8] M. E. van Leeuwen and B. Smit, *Phys. Rev. Lett.* **71**, 3991 (1993).
- [9] M. J. Stevens and G. S. Grest, *Phys. Rev. Lett.* **72**, 3686 (1994).
- [10] I. Szalai, D. Henderson, D. Boda, and K.-Y. Chan, *J. Chem. Phys.* **111**, 337 (1999).
- [11] J. Bartke and R. Hentschke, *Phys. Rev. E* **75**, 061503 (2007).
- [12] R. Hentschke and J. Bartke, *Phys. Rev. E* **77**, 013502 (2008).
- [13] S. C. McGrother and G. Jackson, *Phys. Rev. Lett.* **76**, 4183 (1996).
- [14] P. J. Camp, J. C. Shelley, and G. N. Patey, *Phys. Rev. Lett.* **84**, 115 (2000).
- [15] A. F. Pshenichnikov and V. V. Mekhonoshin, *Eur. Phys. J. E* **6**, 399 (2001).
- [16] G. Ganzenmüller and P. J. Camp, *J. Chem. Phys.* **126**, 191104 (2007).
- [17] N. G. Almarza, E. Lomba, C. Martín, and A. Gallardo, *J. Chem. Phys.* **129**, 234504 (2008).
- [18] Yu. V. Kalyuzhnyi, I. A. Protsykevych, G. Ganzenmüller, and P. J. Camp, *EPL* **84**, 26001 (2008).
- [19] J. Dudowicz, K. F. Freed, and J. F. Douglas, *Phys. Rev. Lett.* **92**, 045502 (2004).
- [20] R. Hentschke, J. Bartke, and F. Pesth, *Phys. Rev. E* **75**, 011506 (2007).
- [21] T. Tlusty, S. A. Safran, *Science* **290**, 1328 (2000).
- [22] W.-Z. Ouyang and R. Hentschke, *J. Chem. Phys.* **127**, 164501 (2007).
- [23] D. C. Rapaport, *The Art of Molecular Dynamics Simulation* (Cambridge University Press, Cambridge, 1995).
- [24] H. J. C. Berendsen, J. P. M. Postma, W. F. van Gunsteren, A. DiNola, and J. R. Haak, *J. Chem. Phys.* **81**, 3684 (1984).
- [25] L. Onsager, *J. Am. Chem. Soc.* **58**, 1486 (1936).
- [26] I. G. Tironi, R. Sperb, P. E. Smith, and W. F. van Gunsteren, *J. Chem. Phys.* **102**, 5451 (1995).

- [27] M. Ley-Koo and M. S. Green, *Phys. Rev. A* **23**, 2650 (1981).
- [28] A. Pelissetto and E. Vicari, *Phys. Rep.* **368**, 549 (2002).
- [29] C. Kriebel, A. Müller, J. Winkelmann, and J. Fischer, *Mol. Phys.* **84**, 381 (1995).
- [30] S. Gupta, *J. Phys. Chem.* **92**, 7156 (1988).
- [31] G. S. Dubey, S. F. ÓShea, and P. A. Monson, *Mol. Phys.* **80**, 997 (1993).
- [32] J. Stoll, J. Vrabec, and H. Hasse, *Fluid Phase Equilib.* **209**, 29 (2003).
- [33] C. Vega, C. McBride, E. de Miguel, F. J. Blas, and A. Galindo, *J. Chem. Phys.* **118**, 10696 (2003).
- [34] Note that the effect of rotational degrees of freedom in systems forming reversible aggregates was first discussed in Ref. [43] in the context of micellar solutions.
- [35] J. A. Barker and D. Henderson, *J. Chem. Phys.* **47**, 4714 (1967).
- [36] P. G. de Gennes and P. A. Pincus, *Phys. Kondens. Mater.* **11**, 189 (1970).
- [37] P. J. Flory, *Principles of Polymer Chemistry* (Cornell University Press, Ithaca, 1953).
- [38] Corrections to this asymptotic behavior at large n are discussed for instance in [44,45].
- [39] R. Hentschke, in *Supramolecular Polymers*, 2nd ed., edited by A. Ciferri (Taylor & Francis, Boca Raton, 2005).
- [40] R. Hentschke, P. Lenz, and B. Fodi, in *Supramolecular Polymers*, edited by A. Ciferri (Taylor & Francis, Boca Raton, 2005).
- [41] P.-G. de Gennes, *Scaling Concepts in Polymer Physics* (Cornell University Press, Ithaca, 1979).
- [42] M. J. Stevens and G. S. Grest, *Phys. Rev. E* **51**, 5976 (1995).
- [43] W. E. McMullen III, W. M. Gelbart, and A. Ben-Shaul, *J. Phys. Chem.* **88**, 6649 (1984).
- [44] H. Frauenkron and P. Grassberger, *J. Chem. Phys.* **107**, 9599 (1997).
- [45] L. V. Yelash, T. Kraska, A. R. Imre, and S. J. Rzoska, *J. Chem. Phys.* **118**, 6110 (2003).